

Na₂V₃O₇, a nanotubular system with spin-1/2 diamond rings

T. Saha-Dasgupta¹, Roser Valentí², F. Capraro², C. Gros³

¹ *S.N. Bose National Centre for Basic Sciences,*

JD Block, Sector 3, Salt Lake City, Kolkata 700098, India

² *Institut für Theoretische Physik, Universität Frankfurt, D-60054 Frankfurt, Germany and*

³ *Department of Physics, University of the Saarland, 66041 Saarbrücken, Germany*

(Dated: February 8, 2020)

Following the recent discussion on the nature of the interactions in the tubular system Na₂V₃O₇, we present a detailed *ab-initio* microscopic analysis of its electronic and magnetic properties. We show by means of a downfolding study that, due to the special geometry of this material, the edge-sharing V-V hopping interactions are of the same order of magnitude as the corner-sharing paths within a ring and an order of magnitude bigger than the hopping interactions between rings in a tube. We propose an effective model in terms of weakly-coupled partially frustrated nine-site rings with the geometry of a spin-diamond necklace. We calculate the susceptibility by exact diagonalization and obtain good agreement with experimental observations.

Introduction- Low-dimensional quantum spin systems, characterized by unconventional magnetic properties, have attracted much attention in the last years¹. A large class of these materials are the spin-1/2 quantum magnets with chain, ladder or planar geometries. Substantial effort has been devoted to the search for new materials with exotic topologies and novel properties and recently, Millet *et. al.*² succeeded in synthesizing the first transition-metal-oxide-based nanotubular system Na₂V₃O₇, a family member of the much discussed NaV₂O₅¹.

The VO₅ pyramids (V's are in nominal valence state 4+) in Na₂V₃O₇ share edges and corners to form a nanotubular structure - a geometry first discovered for carbon- with Na atoms located inside and around each individual tube (see FIG. 1). The complex geometry of the compound is expected to provide non-trivial pathways for the exchange interaction and hence to exhibit a non-trivial magnetic behavior. Initially this compound was predicted to be an example of a $S = 1/2$ nine-leg (or three-leg ladder) system with periodic boundary conditions along the rung direction². Using the extended Hückel method, Whangbo and Koo³ conjectured, on the other hand, that the tubes could be described by six mutually intersecting helical spin chains which should show a gap in the spin excitation spectra.

Antiferromagnetic (AF) spin ladders with even number of legs are expected to show a spin gap and the existence of this gap is not sensitive to the boundary condition along the rung direction. However, in the case of a ladder with an odd number of legs, the topology is important. An odd-leg ladder with open boundary conditions in the rung direction behaves effectively as a $S = 1/2$ AF Heisenberg chain and therefore shows no gap in the spin-excitation spectra. This situation changes dramatically when the boundary condition along the rung direction is periodic, as is the case for the spin tubes in Na₂V₃O₇. The introduction of periodic boundary conditions brings in an additional degree of freedom in the problem, namely the chirality^{4,5} and the ground state is then four-fold degenerate with a gap to the first excited state⁶. However,

the magnetic properties of Na₂V₃O₇ as reported in the literature neither fit the properties of odd-leg spin tubes nor to that of helical spin chains as proposed by Whangbo and Koo³ since no appreciable spin gap could be detected in the susceptibility measurements⁷ - *Na₂V₃O₇ exhibits neither a phase transition to a magnetically ordered state nor spin-freezing phenomena at temperatures above 2 K.* A way out of this puzzling situation has been suggested by Lüscher *et. al.*⁸ by considering frustrated inter-ring couplings within the framework of a three-leg spin tube. While this surely provides a nice model by itself with interesting properties, its relevance for Na₂V₃O₇ system remains yet to be examined.

Even though this compound has generated interest and controversy, no first-principles microscopic study has been reported so far. Our work in that respect is the first microscopic study carried out for Na₂V₃O₇. We have analyzed the *ab-initio* density functional theory (DFT) results in terms of the newly developed N-th order muffin-tin-orbital (NMTO) based downfolding technique⁹ to provide a microscopically-derived spin model for Na₂V₃O₇. Our result shows that the appropriate description of the system is that of nine-site rings with partially frustrated, next-nearest neighbor intra-ring interactions while the rings are very weakly coupled along the tube. Validity of this model is provided by the good agreement of our calculated susceptibility data with the measured data.

Ab-initio Study- Na₂V₃O₇ crystallizes² in the trigonal space group, P31c, with Z=6 and lattice constants $a = 10.89\text{Å}$ and $c = 9.54\text{Å}$. There are three inequivalent V sites - V1, V2, V3, seven inequivalent O sites - O1-O7 and four inequivalent Na sites, Na1- Na4. Each V is surrounded by five oxygen atoms with one characteristic short V-O bond of length in the range 1.63 - 1.64Å and four unequal, long V-O bonds of lengths in the range 1.84 - 2.02Å giving rise to distorted square pyramids. The VO₅ pyramids share edges and corners to form nanotubes with internal diameter of about 5 Å. Na1 atoms sit inside each nanotube while Na2, Na3 and Na4 atoms are situated outside individual nanotubes to form an array

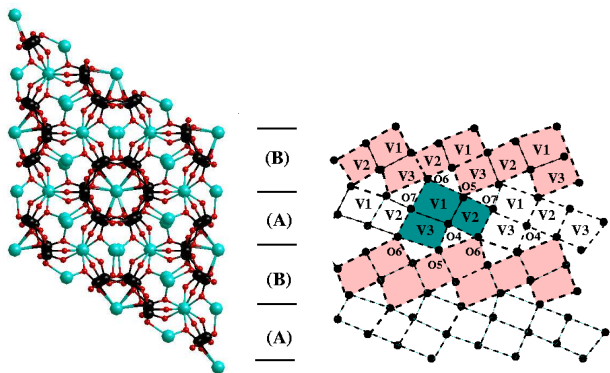


FIG. 1: Crystal structure of $\text{Na}_2\text{V}_3\text{O}_7$. (a) Projection on to the (001) plane. V, Na and O atoms are denoted by black, blue and red balls respectively. (b) Unfolded view of the edge and corner-sharing VO_5 pyramids within a tube along z . The basic V1-V2-V3 unit formed on the basis of short first nearest neighbor V-V distances are marked in dark green.

of such nanotubes arranged in periodic order as shown in FIG. 1(a). The arrangement of VO_5 pyramids in a single tube is better viewed in the unfolded idealized representation of the nanotube as shown in FIG. 1(b) where in addition to inequivalent V atoms, the oxygen atoms have been also denoted. The O1, O2 and O3 atoms, not marked in the figure, are positioned at the apex of VO_5 pyramids centered by V1, V2 and V3 atoms respectively, all of them pointing out of the tube. Considering the short V-V distances, the edge sharing VO_5 pyramids form nine-member rings out of the basic unit V1-V2-V3, in alternating sequence of (V2-V1-V3)-(V2-V1-V3)-(V2-V1-V3) and (V3-V1-V2)-(V3-V1-V2)-(V3-V1-V2) within slices (A) and (B). Rings in slices (A) and (B) are connected to each other by the corner sharing oxygens O5 and O6 to form a nanotube oriented along the z -direction.

The DFT band-structure in the generalized gradient approximation (GGA)¹⁰, calculated using the linearized muffin tin orbital (LMTO) method based on the Stuttgart TBLMTO-47 code¹¹ and the linear augmented plane wave (LAPW)¹² method, consists of primarily oxygen- p and V- d derived bands in the region of interest. The oxygen- p dominated bands are separated by an energy gap of about 3 eV¹³ from the V- d dominated bands. The V- d dominated bands span an energy range of about 4 eV, starting from -0.7 eV to 3.5 eV, with the zero of energy set at the GGA Fermi energy. The pyramidal co-ordination of oxygen atoms surrounding the V atom, sets the V- xy d orbital to be the lowest energy state within the V- d manifold (in the local reference frame, with the z -axis pointing along the short V-O bond). The V- xy bands therefore appear as *essentially* non-bonding set of bands extending from -0.7 eV to 0.4 eV around the Fermi level, with small mixing of oxygen character. The V- xy complex consists of 18 bands, 6 for every V1, V2 and V3 atoms in the unit cell. The crystal-field split V- yz , xz , $3z^2-1$ and x^2-y^2 com-

plexes appear in the energy spectrum above the V- xy complex in order of increasing energy. Na-derived states lie farther high up in energy with practically no mixing to bands close to Fermi energy.

We further analyze the DFT-derived *ab-initio* band-structure result in terms of low-energy, few-orbital model Hamiltonians by employing the downfolding technique within the framework of the N-th order muffin tin orbital method⁹, which has proved to be highly successful in deriving effective model Hamiltonians starting from full LDA/GGA band-structure studies¹⁴. The method relies on designing energy-selective Wannier-like effective orbitals by integrating out degrees of freedom that are not of interest. The few-orbital Hamiltonian is then constructed in the basis of these Wannier-like effective orbitals. Since the degrees of freedom are integrated out, rather than being simply ignored, the method naturally takes into account the renormalization effect coming from orbitals not considered explicitly. In particular, in the present case, we integrate out all the degrees of freedom other than V- xy orbitals to derive a V- xy only few-orbital model Hamiltonian. The effective V- xy muffin tin orbitals (MTO's) generated in the process contains in its tail the integrated out O- p and remaining V- d orbitals, the weight being proportional to their mixing to V- xy derived bands. Fourier transform of the few-orbital Hamiltonian in the *downfolded* V- xy basis gives the tight-binding Hamiltonian, $H_{TB} = -\sum_{\langle i,j \rangle} t_{ij}(c_j^\dagger c_i + c_i^\dagger c_j)$ in terms of dominant V-V effective hopping integrals, t_{ij} , where i and j denote a pair of V^{4+} ions, each one labeled by (n, s, k) where n denotes the unit cell, s the multiplicity ($s=1, \dots, 6$) and k the type ($k = 1, 2, 3$) of V^{4+} ion in the unit cell.

The nearest neighbor (n.n.) V-V interactions within the V1-V2-V3 basic unit (marked by dark green in FIG. 1(b)) proceed via the edge-sharing oxygens while the next nearest neighbor (n.n.n.) interactions proceed via corner-sharing oxygens. The first neighbor shell of V-V pairs formed by edge-sharing $[\text{V}_i\text{O}_k\text{O}_l\text{V}_j]$ complexes are of distances: 2.91\AA for $i = 1, j = 2, k, l = 4, 5$; 2.98\AA for $i = 1, j = 3, k, l = 4, 7$ and 3.06\AA for $i = 2, j = 3, k, l = 6, 7$. The next set of interactions between V-V pairs belonging to the same ring are formed by corner-sharing $[\text{V}_i\text{O}_l\text{V}_j]$ complexes of distances 3.71\AA for $i = 1, j = 2, l = 7$ and 3.55\AA for $i = 2, j = 3, l = 4$. The adjacent rings (*e.g.* rings marked by slices A and B in FIG. 1) are connected by edge-sharing O5 and O6 oxygens. Our first-principles-derived hopping integrals show that the edge-sharing n.n. V-V interactions within the V1-V2-V3 basic unit are of magnitude ranging from -0.14 eV to -0.18 eV. The n.n.n corner sharing intra-ring interactions are nearly equally strong with V1-V2 (V1-V3) interaction being of magnitude -0.14 eV (-0.13 eV). The inter-ring V-V couplings are an order of magnitude weaker compared to intra-ring couplings, -0.03 eV being the strongest of all the inter-ring hoppings, followed by the next strong inter-ring coupling of magnitude -0.01 eV. FIG. 2 shows the various V-V hopping integrals and

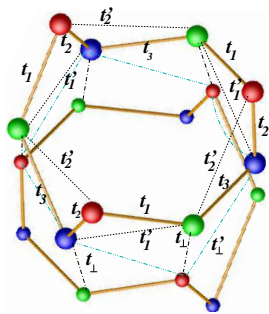


FIG. 2: Hopping parameters corresponding to the tight-binding modeling of $\text{Na}_2\text{V}_3\text{O}_7$. Shown in the picture are two adjacent rings of the nanotube [corresponding to slices (A) and (B) in Fig. 1] viewed from slightly off top. Larger symbols are for the top-most layer vanadiums and the smaller symbols are for bottom layer vanadiums. Red, green and blue circles mark the positions V1, V2 and V3 ions respectively.

TABLE I: Inter and intra-ring hopping integrals in eV. Only hoppings of magnitude larger than and equal to 0.01 eV are shown.

Intra-ring					Inter-ring	
t_1	t_2	t_3	t'_1	t'_2	t_\perp	t'_\perp
-0.18	-0.15	-0.14	-0.13	-0.14	-0.03	-0.01

their actual magnitudes are tabulated in TABLE I.

This result is very different from the extended Hückel molecular-orbital-based result of Whangbo and Koo³ which predicts that coupling via corner-sharing pyramids is much larger than that via edge-sharing for $\text{Na}_2\text{V}_3\text{O}_7$. While this conclusion is in general true for vanadate systems like NaV_2O_5 , LiV_2O_5 and CsV_2O_5 ¹⁵ it fails in the case of $\text{Na}_2\text{V}_3\text{O}_7$. Our result shows that the peculiar geometry of the VO_5 coordination with marked deviation of the V-O-V bond angles from 180° and highly non-coplanar nature of V-O-V bonds, gives rise to coupling via edge-sharing nearly equally strong as that via corner-sharing as long as one is confined to a single ring. The magnitude of intra-ring, edge-sharing couplings are comparable to the largest edge-sharing hopping parameters in other vanadate systems like CsV_2O_5 (-0.12 eV)¹⁶ or LiV_2O_5 (-0.18 eV)¹⁷ while the magnitude of intra-ring, corner-sharing couplings is much smaller than the largest corner-shared V-O-V in LiV_2O_5 or NaV_2O_5 which are about -0.3 eV^{17,18}. The corner-sharing coupling between two adjacent rings is substantially diminished due to further mis-alignment of $V-xy$ orbitals belonging to two different rings which mixes the π character of the bond with that of δ character. In FIG. 3 we show the various *downfolded* $V-xy$ MTO-s and their overlap giving us an idea of the influence of the distorted geometry on the relative orientations of the effective $V-xy$ orbitals, interaction paths and the magnitude of overlaps.

Our analysis shows that $\text{Na}_2\text{V}_3\text{O}_7$ can be described as

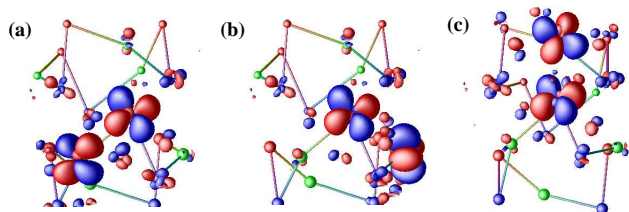


FIG. 3: Various intra-ring and inter-ring overlaps of the *downfolded* $V-xy$ MTO-s. Two different sizes of circles corresponds to V atoms belonging to two different adjacent rings. (a) Edge-sharing intra-ring, nearest-neighbor V1-V2 overlap (b) Corner-sharing intra-ring, second neighbor V1-V2 overlap (c) Inter-ring V1-V2 overlap.

formed by tubes consisting of very weakly coupled nine-site rings with *partial* intra-ring frustration. The *partial* frustration is due to the absence of the second neighbor V1-V3 interaction which is neither corner-sharing nor edge-sharing, rather it is decoupled by the intervening $\text{V2}(\text{O}_5)$ pyramid.

Susceptibility - Our DFT-results, as summarized in TABLE I, indicate nearly independent 9-site rings as the building blocks in $\text{Na}_2\text{V}_3\text{O}_7$. The exchange couplings between the spins, using the perturbative approach, are given by: $J_i \sim 4t_i^2/U$ where t_i correspond to the hoppings via various V-O-V superexchange paths and U is the on-site repulsion with values $U \approx 3-4$ eV, typical for vanadate systems¹. A good guess for an estimate for the exchange coupling can be obtained by considering the *ab initio* t_i 's.

We neglect in the following the small inter-ring couplings and the differences in between the three n.n. interactions. Also, the two n.n.n. interactions will be assumed to be equal since $t'_1 \approx t'_2$. The underlying spin-1/2 Hamiltonian is then given by

$$H = J_1 \sum_{i=1}^9 \left(\vec{S}_i \cdot \vec{S}_{i+1} + \alpha_i \vec{S}_i \cdot \vec{S}_{i+2} \right), \quad (1)$$

with $\alpha_i = J_2^i/J_1$ and periodic boundary conditions $\vec{S}_{L+i} = \vec{S}_i$ ($L=9$). The *ab-initio* result indicates the n.n.n coupling to be inhomogenously distributed in the sense that $\alpha_i = 0$ for $i = 1, 4, 7$ and $\alpha_i \neq 0$ ($=\alpha'$) for $i = 2, 3, 5, 6, 8, 9$ (see left illustration in FIG. 4). For a further check of the goodness of this model we considered in addition the fully frustrated model with $J_2^i = J_2$ for all i ($\alpha_i = \alpha$) (see right illustration in FIG. 4).

In FIG. 4 we present a comparison of the experimentally observed inverse magnetic susceptibility⁷ (filled dots) with the inverse magnetic susceptibility obtained from exact diagonalization of the above-mentioned two kinds of frustrated models, varying the parameters α and α' .

We observe that only the partially frustrated model ($\alpha' \neq 0$), which is the model predicted from the *ab initio* calculations, is able to reproduce the experimental data over the whole range of temperature. The fully

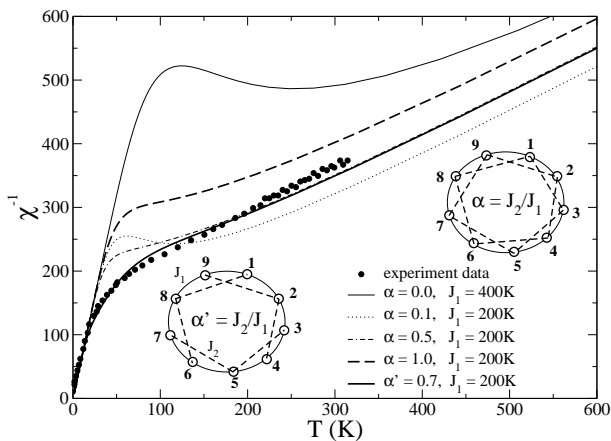


FIG. 4: Temperature dependence of the inverse magnetic susceptibility in units of mol/emu obtained from exact diagonalization for the two frustrated models of the inset (see Eq. (1)) compared with the experimental data⁷ (filled dots).

frustrated model consistently shows an upturn of the inverse susceptibility at lower temperatures not observed experimentally. In FIG. 5 we show in more detail the susceptibility comparison in the low-temperature range for various parameters of the partially frustrated model. The optimal parameters seem to be $J_1 = 200$ K and $J_2 = 140$ K ($\alpha' = 0.7$) within the assumed approximation of $t_1 = t_2 = t_3$ and $t'_1 = t'_2$.

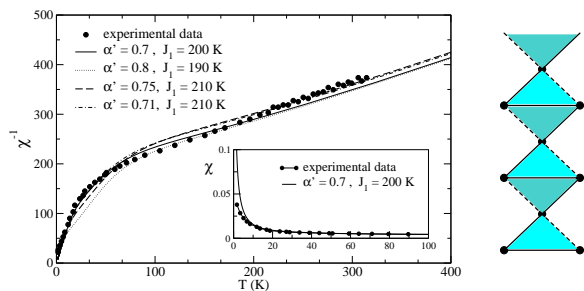


FIG. 5: Left panel: Inverse magnetic susceptibility in units of mol/emu obtained from exact diagonalization for the partially frustrated model for various values of α' compared with the experimental data⁷ (filled dots). In the inset, the temperature dependence of the susceptibility (emu/mol) is shown. Right panel: Illustration of the spin-diamond chain. Full and dashed lines correspond to J_1 and $\alpha'J_1$ bonds respectively, see Eq. (1).

The partially frustrated model is invariant under translations $i \rightarrow i + 3$ ($i = 1, \dots, 9$) and corresponds therefore in the low-energy sector to a three-site ring. The ground state is therefore four-fold degenerate, i.e. it is a chirality-degenerate spin-doublet⁶. The susceptibility of the partially frustrated model therefore diverges at low temperatures as $1/T$ (illustrated in the inset of FIG. 5). Below ~ 10 K the experimental data increases slower than expected for free spin-1/2 moments (one for every nine V-sites), presumably due to residual inter-ring interactions which were not considered in our idealized model.

Our *ab initio* results show that -though very small- there are two contributions to the inter-ring coupling (see TABLE I and FIG. 2) which will be important at low temperatures and can compete against each other. The inter-ring exchange coupling $\sim 4t_{\perp}^2/U$ will generally induce a spin-gap⁶ which will scale with the inter-ring exchange coupling. Recent density matrix renormalization group calculations of Lüscher *et al.*⁸ further showed that the spin gap diminishes if inter-ring frustration is present. The experimental observation of absence of appreciable spin-gap⁷ may be, therefore, rationalized in terms of (i) the smallness of the inter-ring spin-spin interaction (refer to TABLE I) and (ii) the inter-ring frustration between t_{\perp} and t'_{\perp} .

It is worth mentioning here that the partially frustrated model, illustrated on the left side of FIG. 5 is of considerable interest by itself. For $\alpha' = 1$ it is geometrically equivalent to the spin-1/2 diamond chain, which corresponds in the low-energy sector to a mixed spin-1 spin-1/2 chain¹⁹. Mixed spin-1 spin-1/2 chains support both acoustic and optic magnetic excitations and are gapless in the thermodynamic limit²⁰. Our result $\alpha' = 0.7$ indicates that $\text{Na}_2\text{V}_3\text{O}_7$ is close to the spin-diamond geometry. We find that the gap in between the degenerate ground-state Kramers-doublet and the lowest magnetic quartet vanishes for the 9-site ring at $\alpha' = 1.0$.

In summary, we derived an effective spin-model for the tubular $\text{Na}_2\text{V}_3\text{O}_7$ system starting from *ab-initio* calculations. Exact diagonalization of the derived model gives satisfactory description of the experimentally measured susceptibility.

We acknowledge useful discussions with V.N. Muthukumar, J. Richter and F. Mila and the support of the Deutsche Forschungs Gemeinschaft.

¹ see for a review P. Lemmens, G. Güntherodt and C. Gros, Physics Reports **375** 1 (2003).

² P. Millet, J. Y. Henry, F. Mila and J. Galy, J. Solid State

Chem., **147** 676 (1999).

³ M.-H. Whangbo, H.-J. Koo, Solid State Comm. **115**, 675 (2000).

- ⁴ V. Subrahmanyam, Phys. Rev B **50**, 16109 (1994).
- ⁵ H-T Wang, Phys. Rev B, **64**, 174410 (2001).
- ⁶ K. Kawano and M. Takahashi, Jour. Phys. Soc. Jap. **66**, 4001 (1997).
- ⁷ J. L. Gavilano, D. Rau, S. Mushkolaj, H. R. Ott, P. Millet, and F. Mila, Phys. Rev. Lett. **90**, 167202 (2003).
- ⁸ A. Lüscher, R. M. Noack, G. Misguich, V. N. Kotov, and F. Mila, cond-mat/0405131
- ⁹ O.K. Andersen and T. Saha-Dasgupta, Phys. Rev. **B62**, R16219 (2000) and references there in.
- ¹⁰ J.P. Perdew, S. Burke, and M. Ernzerhof, Phys. Rev. Lett. **77**, 3865 (1996).
- ¹¹ O. K. Andersen, Phys. Rev. B, **12**, 3060 (1975).
- ¹² P. Blaha, K. Schwarz, G. K. H. Madsen, D. Kvasnicka and J. Luitz, WIEN2k, 2001. ISBN 3-9501031-1-2
- ¹³ We checked convergence of the band-structure results obtained with the TB-LMTO scheme -where the downfolding procedure is implemented- versus the results from the full potential LAPW scheme.
- ¹⁴ See references in O. K. Andersen, T. Saha-Dasgupta and S. Ezhov, Bull. of Mater. Sci. **26** 19 (2003).
- ¹⁵ Y. Ueda, Chem. Mater. **10**, 2653 (1998).
- ¹⁶ R. Valentí and T. Saha-Dasgupta, Phys. Rev B, **65**, 144445 (2002).
- ¹⁷ R. Valentí, T. Saha-Dasgupta, J.V. Alvarez, K. Pozgajcic, C. Gros, Phys. Rev. Lett. **86**, 5381, (2001).
- ¹⁸ V. V. Mazurenko, A. I. Lichtenstein, M. I. Katsnelson, I. Dasgupta, T. Saha-Dasgupta, and V. I. Anisimov, Phys. Rev. B **66**, 081104(R) (2002).
- ¹⁹ N. Fukushima, A. Honecker, S. Wessel and W. Brenig, Phys. Rev. B **69**, 174430 (2004).
- ²⁰ S. K. Pati, S. Ramasesha and D. Sen, Phys. Rev. B **55**, 8894 (1997).